Biased Borate Esterification during Nucleoside Phosphorylase-Catalyzed Reactions: Apparent Equilibrium Shifts and Kinetic Implications

Felix Kaspar,[a,b,#] * Felix Brandt,[c,#] Sarah Westarp,[b,d] Lea Eilert,[a,e] Sebastian Kemper,[f] Anke Kurreck,[b,d] Peter Neubauer,[b] Christoph R. Jacob,[c] and Anett Schallmey[a]

[a] Institute for Biochemistry, Biotechnology and Bioinformatics, Technische Universität Braunschweig, Spielmannstraße 7, 38106, Braunschweig, Germany, felix.kaspar@tu-bs.de / felix.kaspar@web.de.
[b] Chair of Bioprocess Engineering, Institute of Biotechnology, Faculty III Process Sciences, Technische Universität Berlin, Straße des 17. Juni 135, 10623, Berlin, Germany.
[c] Institute of Physical and Theoretical Chemistry, Technische Universität Braunschweig, Gaußstraße 17, 38106 Braunschweig, Germany.
[d] BioNukleo GmbH, Ackerstraße 76, 13355 Berlin, Germany.
[e] present address: Department Structure and Function of Proteins, Helmholtz Centre for Infection Research, Inhoffenstraße 7, 38124 Braunschweig, Germany.
[f] Institute for Chemistry, Technische Universität Berlin, Straße des 17. Juni 135, 10623 Berlin, Germany
[#] These authors contributed equally.

Biocatalytic nucleoside (trans-)glycosylations catalyzed by nucleoside phosphorylases have graduated to a practical and convenient approach to the preparation of modified nucleosides, which are important pharmaceuticals for the treatment of various cancers and viral infections. However, the obtained yields in these reactions are generally determined exclusively by the innate thermodynamic properties of the nucleosides involved, hampering the biocatalytic access to many sought-after target nucleosides. We herein report an orthogonal dimension for reaction engineering of these systems. We show how apparent equilibrium shifts in phosphorolysis and glycosylation reactions can be effected through entropically driven, biased esterification of nucleosides with inorganic borate. Our multifaceted analysis further describes the kinetic implications of this in situ reactant esterification for a model phosphorylase. Our results suggest an unusual pseudo-non-competitive inhibitory mechanism where reversible binding of the borate ester of the nucleoside substrate yields a non-productive inhibitor-enzyme complex. This complex exhibits constricted molecular dynamics and exists in a rapid equilibrium with the productive enzyme-substrate complex via hydrolytic interconversion. Collectively, this report presents a partial departure from the stringent thermodynamic constraints of nucleoside phosphorolysis reactions and shines light on the molecular processes regulating the activity of nucleoside-binding enzymes in the presence of borate.

Nucleosides and their analogs are central to the biological and chemical sciences, as they serve a variety of biological functions and represent a growing class of anti-cancer and anti-viral pharmaceuticals.[1] Although the synthesis of nucleosides typically proceeds *via* *N*-glycosylation of nucleobases with heavily protected sugar synthons, there is an increasing recognition for the inefficiency of the associated synthetic routes.[2] Consequently, recent years have experienced renewed interest in the biocatalytic synthesis of natural and modified nucleosides. This includes, for instance, the enzymatic preparation of halogenated purine nucleoside synthons,[3] the diversification of alkylated pyrimidine nucleoside analogues,[4] the development of high-yielding flow processes,[5] and the synthesis of the pharmaceuticals islatravir (anti-HIV)[6] and molnupiravir (anti-Covid19)[7] in biocatalytic cascades. All these examples employ nucleoside phosphorylases for key (trans-)glycosylation reactions, which enable the installation of ribosyl-based moieties on pyrimidine and purine nucleobases in one step and without the need for any protecting group chemistry.

Nucleoside phosphorylases catalyze the reversible phosphorolysis of nucleosides to the corresponding nucleobases and pentose-1-phosphates (Scheme 1).[8] This reactivity can be employed in reverse to transfer the glycosyl moiety from one nucleoside (or a pentose-1-phosphate) to another nucleobase, a reaction typically referred to as a (trans-)glycosylation.[9] While such (trans-)glycosylation processes are well established as synthetic tools,[10–19] they inherently suffer from thermodynamic limitations, as the final yield of these reactions is dictated solely by the substrate-dependent thermodynamics of the respective (reverse) phosphorolytic steps as well as the employed reaction conditions.[9,20,21] Although some progress has been made to mitigate or exploit the tight thermodynamic control in these systems (e.g., *via* (by)product precipitation,[22] enzymatic product removal[23] or application of recoverable excess

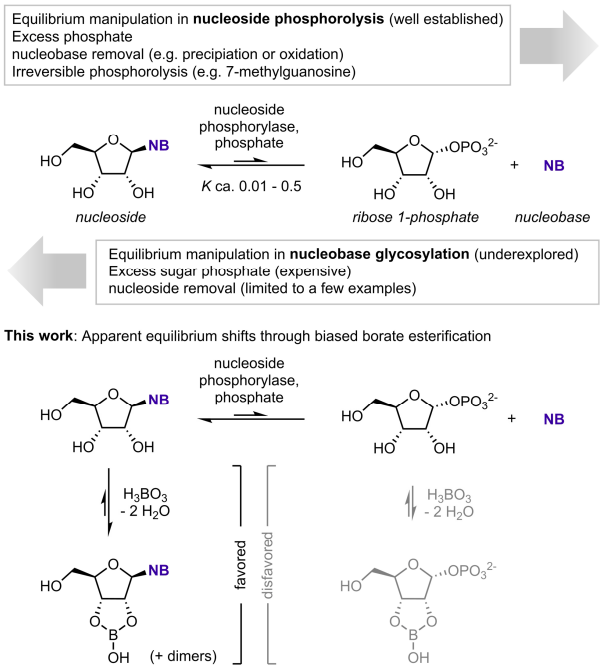

Scheme 1. Nucleoside phosphorolysis and strategies for apparent equilibrium shifts. NB = nucleobase.

reagent[24]) and irreversible phosphorolysis of 6-oxopurines is well established,[10,25,26] there currently exists no general method for the direct manipulation of glycosylation equilibria.

During our development of the PUB module for continuous high-throughput phosphate detection in biochemical assays,[27] we serendipitously found that the presence of borate effects a series of inhibitory phenomena during pyrimidine nucleoside phosphorolysis as well as an apparent equilibrium shift caused by biased borate esterification of nucleosides over ribose 1-phosphate (**Rib1P**). While saccharides are well known to undergo complex equilibrium reactions with borate in aqueous solution,[28,29] comparably little is known about *in situ* competition of such processes. Similarly, although the literature offers some examples for biocatalytic applications of equilibrium shift phenomena through preferential esterification of one reactant with borate (namely, the enzymatic epimerization of fructose,[30] lactose,[31] galactose,[32,33] and arabinose[34]) the exact species involved in these processes remain largely elusive, as do the kinetic implications of this esterification on the enzyme-level. Despite the precedents for borate inhibiting NAD^+-dependent enzymes in a non-competitive fashion,[35,36] the molecular determinants and mechanisms of these phenomena have remained equally elusive. To shed light on the thermodynamic and kinetic implications of borate ester formation on nucleoside phosphorylase-catalyzed reactions, we herein report a multifaceted analysis of this reaction system with spectroscopic and computational approaches. Furthermore, we examined the synthetic utility of this biased borate esterification, as concentration-dependent apparent equilibrium shifts provide an orthogonal dimension for reaction engineering in biocatalytic glycosylation reactions.

Our investigation was sparked by the serendipitous observation that phosphorolysis reactions with 5-bromouridine (**1a**) consistently exhibited noticeably lower equilibrium conversions in the presence of moderate concentrations of borate (Figures 1A and B). For instance, a reaction containing 400 µM **1a**, 4 mM (10 equivalents) phosphate and 40 µg mL^{-1} (0.45 mol%) of the well characterized pyrimidine nucleoside phosphorylase from *Geobacillus thermoglucosidasius* (*Gt*PyNP),[4,37–40] serving as a model enzyme (see the Supplementary Information for details), reached its equilibrium at 70% conversion after 10 min in glycine-buffered solution (Fig. 1B). In contrast, the same reaction additionally containing 20 mM borate took almost 20 min to reach an equilibrium at 47% conversion, as monitored by multi-wavelength UV spectroscopy employing principles of spectral unmixing.[41,42] This effect was not rooted in enzyme inactivation, as *Gt*PyNP showed an identical melting point and fully retained its catalytic activity after prolonged incubation in borate-containing buffers (Figs. S1 and S2). The observed apparent equilibrium shift persisted in the reverse direction of the reaction (starting from the products **Rib1P** and **2a**, Fig. S6) and additional experiments established that the reaction system consistently behaved according to lower apparent equilibrium constants of phosphorolysis (*K'*), whose magnitude depended on the concentration of borate (Fig. 1C). Since such drastic equilibrium shifts are unprecedented for phosphorolysis systems, we suspected that the formation of a dominant secondary species would actively remove the nucleoside **1a** from this equilibrium in a thermodynamically controlled fashion. Indeed, the conversion data phenotypically following a Boltzmann-type relationship (Fig. 1D) could be described

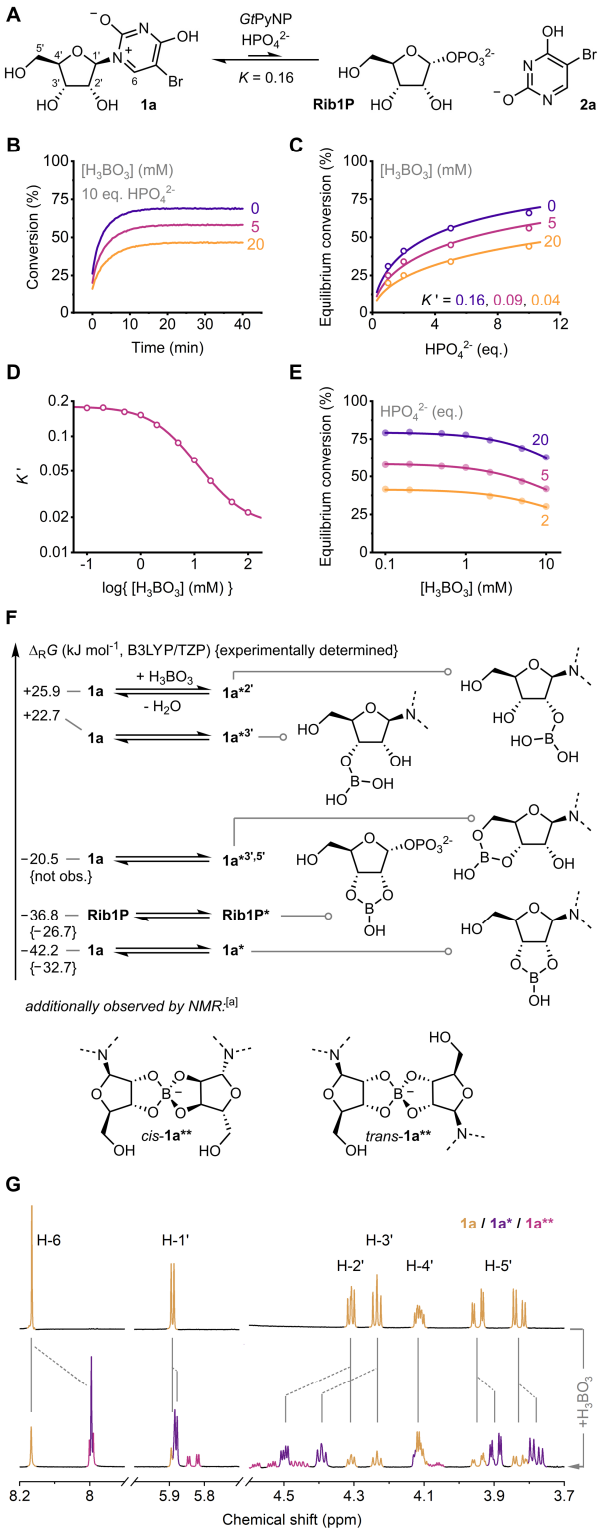

Figure 1. A Phosphorolysis of 5-bromouridine (**1a**), and **B**–**E** apparent equilibrium shifts observed in the presence of borate. **F** DFT data. **G** ^1H NMR of **1a** (10 mM) with or without 20 mM borate in 200 mM glycine buffer at pH 9 and 25 °C. See the SI for experimental details, raw data and equations.[43] [a] Not confidently accessible by DFT due to their high charge.

well with a thermodynamic model accounting for the presence of an additional equilibrium system in which **1a** is partially transformed to a borate ester (Fig. 1E, see the SI for details and equations). Although borate esters of ribose are known to persist in dilute aqueous solution,[44–46] these stable esters generally involve the anomeric hydroxyl group, which is absent in **1a**. Nevertheless, Kim *et al.*[47,48] observed borate esters of the nucleoside-based cofactor NAD^+ and the natural trinucleotides by mass spectrometry, indicating that analogous species might be formed by recruitment of the 2′- and/or 3′-hydroxyl groups. In addition, structurally similar nucleoside boronate esters have been reported by Smietana[49,50] and others.[51] Based on these precedents, we hypothesized that the cyclic borate ester **1a*** would be the predominant species causing the observed equilibrium shift (Fig. 1F).

To probe if borate esters like **1a*** would be feasible species to effect apparent equilibrium shifts under dilute aqueous reaction conditions, we turned to density functional theory (DFT) calculations and NMR spectroscopy. DFT calculations (using B3LYP/TZP[52–55] in combination with a COSMO[56] solvent model for water, see the SI for details) suggested that the formation of the 2′- or 3′-borate monoesters of **1a** would be highly disfavored processes, while the formation of the proposed five-membered cyclic diester **1a*** offers around 40 kJ mol^{-1} net gain in Gibbs free energy, indicating that this esterification could feasibly proceed against the concentration gradient of water (Fig. 1F). Indeed, direct evidence for the presence of **1a*** could be obtained by NMR spectroscopy. When **1a** (10 mM) was incubated with 20 mM borate in glycine buffer at pH 9, a dominant borate-containing species in equilibrium with free borate could be observed by ^{11}B NMR (Fig. S10), while ^1H NMR showed additional signals indicative of a modification of the ribosyl moiety of **1a** (Fig. 1G). Furthermore, slight changes in the coupling constants across the sugar ring implied the introduction of ring torsion, consistent with the configurational changes required in **1a*** (Table S4). In addition to this ester, we observed two distinct minor components in the mixture, which exhibited identical coupling constants to **1a*** and existed in similar concentrations (ca. 1:1.2 ratio). Based on the well-characterized diastereomeric borate ester dimers of methyl apiose described by Ishii and Ono[57] and the report of purine nucleoside solubilization as 2:1 complexes with borate by Tsuji and colleagues,[58] we tentatively ascribe these species as the *cis*- and *trans*-isomers **1a**** (Figs. 1G and F). Overall, the Gibbs free energies obtained experimentally by NMR spectroscopy or equilibrium state calculations based on UV data ($\Delta_R G$ ca. −32 kJ mol^{-1}, see the SI for details) are comparable to those obtained by DFT calculation. Although an analogous six-membered ester (and potentially its dimers) between the 3′- and 5′-hydroxyl groups would introduce similar configurational changes to those ascribed to **1a***, DFT calculations revealed that its formation is much less exothermic and consequently disfavored. Similarly, the analogous five-membered borate ester of **Rib1P** is less favored than **1a*** (which is requisite for the observed equilibrium shift), as supported by DFT and NMR data (Figs. 1F and S10). Additionally, we observed no trace of dimers of **Rib1P*** by NMR, which is likely a result of the highly disfavored formal −5 charge of these species. Consequently, the formation of the borate ester **1a*** should be expected to dominate in direct competition during a phosphorolysis reaction, which we could confirm by subjecting phosphorolysis reaction mixtures with increasing borate concentrations to NMR analysis (Fig. S13). Further thermodynamic experiments indicated that this biased esterification is primarily driven by entropic effects. Arrhenius plots of the **1a**-**1a*** equilibrium obtained by ^1H NMR revealed a drastic temperature-dependence, favoring the presence of the free nucleoside at higher temperatures (Fig. S11). In support of these observations, Arrhenius plots for the borate esterification derived from equilibrium shifts in the phosphorolysis reaction indicated an approach to an energetic balance between **1a*** and **Rib1P*** at higher temperatures (Fig. S5). Collectively, these results describe **1a*** as the dominant borate ester in this reaction system, responsible for depleting the pool of free nucleoside in dilute aqueous solution at room temperature. Consistent with this conclusion, the 2′-deoxy nucleoside **deoxy-1a**, incapable of forming **1a*** or **1a****, did not show an equilibrium shift during its phosphorolysis in the presence of borate or any reaction with borate discernible by NMR (Fig. S15).

Next, we sought to identify the cause of the apparently reduced reaction rates in the presence of borate by enlisting kinetic studies and molecular dynamics (MD) simulations. This effect was especially prominent with borate concentrations greater than 20 mM and led to decreases in the reaction rate of *Gt*PyNP by more than a factor of four, as illustrated in Figure 2D. Since high borate concentrations primarily yield **1a*** in solution (and not the enzymatic substrate **1a**), we initially entertained the hypothesis that this phenomenon was a function of the decreased concentration of the free nucleoside substrate and the associated apparent decrease of affinity. However, the Michaelis-Menten kinetics obtained for **1a** (with phosphate in excess) proved inconsistent with this hypothesis. While a reduction in available substrate concentration should primarily result in a decrease in the apparent Michaelis-Menten constant K_M, we observed no change in K_M but instead a sharp decline of the rate constant under saturating substrate concentrations (k_{cat}, Fig. 2B). With saturating concentrations of both substrates, the observed rate constant k_{obs} exhibited a similar Boltzmann-type decrease as observed for the apparent equilibrium constant, which could be described well by an equilibrium model expressing the observed rate constant as a function of k_{cat} and the esterified fraction of **1a** (Fig 2D, see the SI for equations). As this decrease of k_{obs} was further completely absent for **deoxy-1a** in the presence of borate (Figs. 2C and E), we concluded that borate alone does not inhibit *Gt*PyNP, but rather the borate ester **1a***. If *Gt*PyNP could bind but not convert **1a***, we reasoned that the position of the equilibrium between **1a** and **1a*** would determine the ratio of potentially active enzyme (**1a** bound to *Gt*PyNP) *versus* inactive enzyme (**1a*** bound to *Gt*PyNP), assuming that catalysis is a rate-limiting step. Given the highly solvent-exposed active site of pyrimidine nucleoside phosphorylases in the open state, we expected that *Gt*PyNP should be able to accommodate the slightly twisted and sterically more demanding borate ester **1a*** and allow its equilibration with the free nucleoside substrate **1a** while bound to the enzyme. Phenomenologically, such a process would resemble a classical non-competitive inhibition, consistent with our kinetic data. Indeed, MD simulations (using GROMACS[59,60] with the CHARMM36[61] force field) based on our recently disclosed crystal structure of *Gt*PyNP in complex with uridine (PDB ID 7m7k,[4] see the SI for details) yielded several insights in support of the proposed model. First, an analysis of the clustered states over 50 ns simulation time

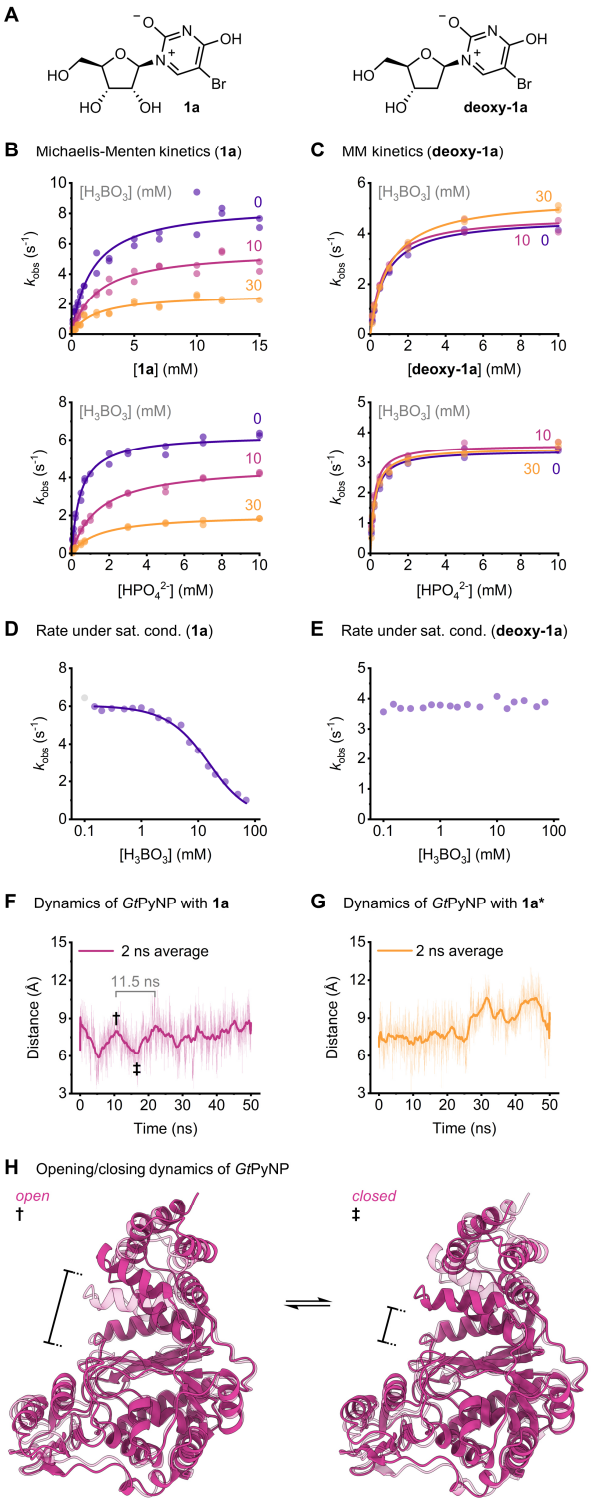

Figure 2. A–C Michaelis-Menten plots of the phosphorolysis of **1a** and **deoxy-1a**, **D** and **E** phosphorolysis rate under saturating conditions. **F–H** MD simulations of *Gt*PyNP with bound **1a** or **1a***. See the SI for experimental details, raw data and equations.[43]

indicates that the borate ester **1a*** can be bound in analogy to **1a** *via* hydrogen bonds with the amide motif of the nucleobase. Secondly, this analysis also showed that the average state in which the enzyme-**1a** and the enzyme-**1a*** complexes resided during the simulation time displayed a quite solvent-exposed active site, feasibly permitting esterification and hydrolysis processes to happen *in situ*. Thirdly, an examination of the distances between the domains responsible for active site closure indicated markedly reduced molecular motion of the enzyme-**1a*** complex compared to the enzyme-**1a** complex (Figs. 2F–H and S19). While *Gt*PyNP with bound **1a** exhibited oscillatory opening and closing motions on a timescale of around 11 ns (similar dynamics are known for the closely related thymidine phosphorylases),[62–68] binding of **1a*** largely arrested this process. Specifically, binding of **1a*** locks the enzyme in an open conformation by displacing a catalytically essential arginine residue, which reversibly adopts an inward position. This appears to halt domain movement and yield an inactive enzyme, while the esterification of the 2'- and 3'-OH groups of **1a** further obstructs access to the anomeric carbon, collectively preventing productive phosphorolysis. As indicated by the clustered structures, **1a*** also slightly obstructs access to the phosphate binding site of *Gt*PyNP. Accordingly, we experimentally observed a decreased affinity for phosphate in the presence of **1a***, in addition to the lower k_{cat} values stemming from pseudo-non-competitive inhibition by **1a*** (Fig. 2B). Experimentally accessed and computed rate constants for the various processes involved in the catalytic cycle also proved consistent with the hypothesized mechanism. Enzyme opening/closing (ca. 0.1 ns^{-1}) occurs on a much shorter time scale than the esterification of **1a** (ca. 3 s^{-1}, Fig. S12), catalysis (ca. 6 s^{-1}) and substrate binding by *Gt*PyNP (ca. 16 s^{-1}, see the SI). Thus, the comparably slow substrate release (ca. 0.2 s^{-1}) necessitates *in situ* hydrolysis of **1a*** to maintain the observed kinetics. In contrast to the phosphorolysis, the kinetics in the glycosylation direction remained essentially unchanged in the presence of borate (Figs. S7 and S8), providing further support for the minor role of **Rib1P*** in this reaction system. Consistent with the entropically driven formation of **1a*** from **1a**, we observed decreased inhibition of the phosphorolysis reaction at higher temperatures, as evident from Eyring plots obtained with different borate concentrations (Fig. S9). Taken together, these results support an inhibitory mechanism phenotypically resembling a non-competitive inhibition, where rapid equilibration of **1a** to its borate ester **1a*** (both in solution and while bound to the enzyme) reversibly decreases the fraction of catalytically active *Gt*PyNP so that throughput in its catalytic cycle is primarily regulated by the position of the **1a**-**1a*** equilibrium (Scheme 2). Preliminary data for other pyrimidine nucleoside phosphorylases as well as other nucleosides suggests that this inhibitory mechanism is likely not limited to *Gt*PyNP and **1a** (Figs. S1 and S18).

With a good understanding of the underlying processes governing the kinetics and thermodynamics of the phosphorolysis of **1a** in the presence of borate, we aimed to apply the observed equilibrium shifts to other nucleosides, specifically targeting glycosylation reactions. Assuming that other nucleosides would behave in analogy to our model compound **1a**, we expected that conversion shifts in glycosylation reactions would provide a general strategy to improve access to nucleosides from the precursor **Rib1P** (which could either be supplied as an isolated compound or generated *in situ*).[10,69–71] Indeed, DFT calculations for a

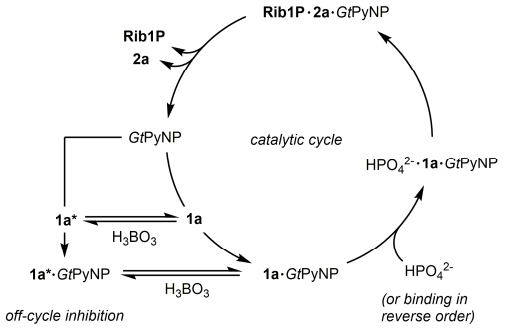

Scheme 2. Proposed mechanism for rate decreases in the presence of borate.

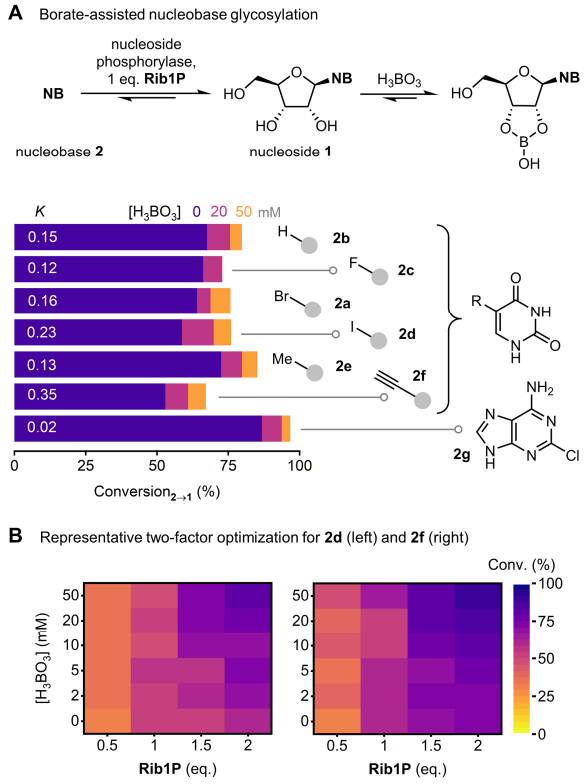

Figure 3. Glycosylation experiments in the presence of borate. *K* refers to the equilibrium constant of phosphorolysis, taken from ref [20].

representative set of nucleosides suggested that a variety of pyrimidine and purine nucleosides should undergo similar esterifications with borate as **1a** (Table S9), which could be confirmed by ^{1}H NMR ($\Delta_R G$ ca. −32 to −34 kJ mol^{-1}, Fig. S14) and, for two examples, with kinetic experiments (see the SI and Fig. S18 for details). Although we were unable to translate the observed minor differences in Gibbs free energies to conversion shifts in transglycosylations, presumably due to a "kinetic lock" effect (see the SI and Fig. S17 for details), glycosylation reactions with various pyrimidine nucleobases **2a**−**f** nicely reflected the expected behavior and facilitated conversion shifts of 6−17% in favor of the respective nucleoside (Fig. 3A). A similar effect could be observed for the halogenated purine **2g** when subjected to identical conditions with the promiscuous purine nucleoside phosphorylase from *G. thermoglucosidasius*. Lastly, an illustrative two-factor optimization for the glycosylation of 5-iodouracil (**2d**) and 5-ethynyluracil (**2f**, both are known for their unfavorable glycosylation thermodynamics)[9,20] showed how a balance of excess sugar donor and the "pull" effect of the corresponding nucleoside borate ester can be employed to improve the conversions in historically challenging nucleobase glycosylations (Fig. 3B). For instance, when using 2 eq. of **Rib1P**, the conversion of **2f** to its nucleoside **1f** could be improved from 74% to 89% through the application of 50 mM borate, which, conventionally, would have required the application of at least 6 eq. of **Rib1P**.

In conclusion, we characterized the equilibrium between ribosyl nucleosides and their corresponding 2′,3′-borate esters in aqueous solution, a phenomenon which facilitates apparent equilibrium shifts during nucleoside phosphorolysis and glycosylation reactions due to a biased esterification of nucleosides over the sugar phosphate **Rib1P**. This borate esterification also causes decreases of the phosphorolysis rate by pyrimidine nucleoside phosphorylases, most likely *via* non-productive binding of the nucleoside borate ester to the enzyme and its hydrolytic interconversion to the free substrate. Collectively, the effects described herein shine light on the activity of nucleoside-binding enzymes in the presence of borate and provide an orthogonal dimension for reaction engineering in nucleobase glycosylation reactions.

Acknowledgements

The authors thank the NMR department of the TU Braunschweig as well as Samantha Voges (TU Berlin) for assistance with spectroscopic experiments and Dr. M. Rhia. L. Stone (Rutgers University) for comments on the manuscript. F.K. gratefully acknowledges funding by the Deutsche Forschungsgemeinschaft (DFG, German Research Foundation), project number 492196858.

Conflict of Interest

The authors declare no conflict of interest.

Author Information

Corresponding Author

Dr. Felix Kaspar,
felix.kaspar@tu-bs.de / felix.kaspar@web.de,
orcid.org/0000-0001-6391-043X

Other Authors

Felix Brandt, orcid.org/0000-0003-2200-5649
Sarah Westarp, orcid.org/0000-0001-6498-8810
Lea Eilert, orcid.org/0000-0002-4753-1322
Dr. Sebastian Kemper, orcid.org/0000-0003-0192-518X
Dr. Anke Kurreck, orcid.org/0000-0001-6919-725X
Dr. Peter Neubauer, orcid.org/0000-0002-1214-9713
Dr. Christoph R. Jacob, orcid.org/0000-0002-6227-8476
Dr. Anett Schallmey, orcid.org/0000-0002-6670-0574

References

(1) Jordheim, L. P.; Durantel, D.; Zoulim, F.; Dumontet, C. Advances in the Development of Nucleoside and Nucleotide Analogues for Cancer and Viral Diseases. *Nat. Rev. Drug Discov.* **2013**, *12*, 447–464. https://doi.org/10.1038/nrd4010.

(2) Kaspar, F.; Stone, M. R. L.; Neubauer, P.; Kurreck, A. Route Efficiency Assessment and Review of the

Synthesis of β-Nucleosides via N-Glycosylation of Nucleobases. *Green Chem.* **2021**, *23*, 37–50. https://doi.org/10.1039/D0GC02665D.

(3) Yehia, H.; Westarp, S.; Röhrs, V.; Kaspar, F.; Giessmann, T. R.; Klare, F. T. H.; Paulick, K.; Neubauer, P.; Kurreck, J.; Wagner, A. Efficient Biocatalytic Synthesis of Dihalogenated Purine Nucleoside Analogues Applying Thermodynamic Calculations. *Molecules* **2020**, *25* (4), 934. https://doi.org/10.3390/molecules25040934.

(4) Kaspar, F.; Seeger, M.; Westarp, S.; Köllmann, C.; Lehmann, A.; Pausch, P.; Kemper, S.; Neubauer, P.; Bange, G.; Schallmey, A.; Werz, D. B.; Kurreck, A. Diversification of 4'-Methylated Nucleosides by Nucleoside Phosphorylases. *ACS Catal.* **2021**, *11* (17), 10830–10835. https://doi.org/10.1021/acscatal.1c02589.

(5) Benítez-Mateos, A. I.; Paradisi, F. Sustainable Flow-Synthesis of (Bulky) Nucleoside Drugs by a Novel and Highly Stable Nucleoside Phosphorylase Immobilized on Reusable Supports. *ChemSusChem* **2022**, *15* (1), e202102030. https://doi.org/https://doi.org/10.1002/cssc.202102030.

(6) Huffman, M. A.; Fryszkowska, A.; Alvizo, O.; Borra-Garske, M.; Campos, K. R.; Canada, K. A.; Devine, P. N.; Duan, D.; Forstater, J. H.; Grosser, S. T.; Halsey, H. M.; Hughes, G. J.; Jo, J.; Joyce, L. A.; Kolev, J. N.; Liang, J.; Maloney, K. M.; Mann, B. F.; Marshall, N. M.; McLaughlin, M.; Moore, J. C.; Murphy, G. S.; Nawrat, C. C.; Nazor, J.; Novick, S.; Patel, N. R.; Rodriguez-Granillo, A.; Robaire, S. A.; Sherer, E. C.; Truppo, M. D.; Whittaker, A. M.; Verma, D.; Xiao, L.; Xu, Y.; Yang, H. Design of an in Vitro Biocatalytic Cascade for the Manufacture of Islatravir. *Science (80-.).* **2019**, *366* (6470), 1255–1259. https://doi.org/10.1126/science.aay8484.

(7) McIntosh, J. A.; Benkovics, T.; Silverman, S. M.; Huffman, M. A.; Kong, J.; Maligres, P. E.; Itoh, T.; Yang, H.; Verma, D.; Pan, W.; Ho, H.-I.; Vroom, J.; Knight, A. M.; Hurtak, J. A.; Klapars, A.; Fryszkowska, A.; Morris, W. J.; Strotman, N. A.; Murphy, G. S.; Maloney, K. M.; Fier, P. S. Engineered Ribosyl-1-Kinase Enables Concise Synthesis of Molnupiravir, an Antiviral for COVID-19. *ACS Cent. Sci.* **2021**, *7* (12), 1980–1985. https://doi.org/10.1021/acscentsci.1c00608.

(8) Kamel, S.; Yehia, H.; Neubauer, P.; Wagner, A. Enzymatic Synthesis of Nucleoside Analogues by Nucleoside Phosphorylases. In *Enzymatic and Chemical Synthesis of Nucleic Acid Derivatives*; Wiley Online Books; 2019; pp 1–28. https://doi.org/10.1002/9783527812103.ch1.

(9) Kaspar, F.; Giessmann, R. T.; Hellendahl, K. F.; Neubauer, P.; Wagner, A.; Gimpel, M. General Principles for Yield Optimization of Nucleoside Phosphorylase-Catalyzed Transglycosylations. *ChemBioChem* **2020**, *21*, 1428–1432. https://doi.org/10.1002/cbic.201900740.

(10) Alexeev, C. S.; Drenichev, M. S.; Dorinova, E. O.; Esipov, R. S.; Kulikova, I. V; Mikhailov, S. N. Use of Nucleoside Phosphorylases for the Preparation of 5-Modified Pyrimidine Ribonucleosides. *Biochim. Biophys. Acta - Proteins Proteomics* **2020**, *1868* (1), 140292. https://doi.org/10.1016/j.bbapap.2019.140292.

(11) Serra, I.; Bavaro, T.; Cecchini, D. A.; Daly, S.; Albertini, A. M.; Terreni, M.; Ubiali, D. A Comparison between Immobilized Pyrimidine Nucleoside Phosphorylase from Bacillus Subtilis and Thymidine Phosphorylase from *Escherichia Coli* in the Synthesis of 5-Substituted Pyrimidine 2′-Deoxyribonucleosides. *J. Mol. Catal. B Enzym.* **2013**, *95*, 16–22. https://doi.org/10.1016/j.molcatb.2013.05.007.

(12) Zhou, X.; Szeker, K.; Jiao, L.-Y.; Oestreich, M.; Mikhailopulo, I. A.; Neubauer, P. Synthesis of 2,6-Dihalogenated Purine Nucleosides by Thermostable Nucleoside Phosphorylases. *Adv. Synth. Catal.* **2015**, *357* (6), 1237–1244. https://doi.org/10.1002/adsc.201400966.

(13) Drenichev, M. S.; Alexeev, C. S.; Kurochkin, N. N.; Mikhailov, S. N. Use of Nucleoside Phosphorylases for the Preparation of Purine and Pyrimidine 2′-Deoxynucleosides. *Adv. Synth. Catal.* **2018**, *360* (2), 305–312. https://doi.org/10.1002/adsc.201701005.

(14) Ubiali, D.; Serra, C. D.; Serra, I.; Morelli, C. F.; Terreni, M.; Albertini, A. M.; Manitto, P.; Speranza, G. Production, Characterization and Synthetic Application of a Purine Nucleoside Phosphorylase from *Aeromonas Hydrophila*. *Adv. Synth. Catal.* **2012**, *354* (1), 96–104. https://doi.org/10.1002/adsc.201100505.

(15) Calleri, E.; Cattaneo, G.; Rabuffetti, M.; Serra, I.; Bavaro, T.; Massolini, G.; Speranza, G.; Ubiali, D. Flow-Synthesis of Nucleosides Catalyzed by an Immobilized Purine Nucleoside Phosphorylase from *Aeromonas Hydrophila*: Integrated Systems of Reaction Control and Product Purification. *Adv. Synth. Catal.* **2015**, *357* (11), 2520–2528. https://doi.org/10.1002/adsc.201500133.

(16) Eletskaya, B. Z.; Gruzdev, D. A.; Krasnov, V. P.; Levit, G. L.; Kostromina, M. A.; Paramonov, A. S.; Kayushin, A. L.; Muzyka, I. S.; Muravyova, T. I.; Esipov, R. S.; Andronova, V. L.; Galegov, G. A.; Charushin, V. N.; Miroshnikov, A. I.; Konstantinova, I. D. Enzymatic Synthesis of Novel Purine Nucleosides Bearing a Chiral Benzoxazine Fragment. *Chem. Biol. Drug Des.* **2019**, *93* (4), 605–616. https://doi.org/10.1111/cbdd.13458.

(17) Kalckar, H. M. The Enzymatic Synthesis of Purine Ribosides. *J. Biol. Chem.* **1947**, *167* (2), 477–486.

(18) Kalckar, H. M. Enzymatic Synthesis of a Nucleoside. *J. Biol. Chem.* **1945**, *158* (3), 723–724.

(19) Friedkin, M.; Kalckar, H. M. Desoxyribose-1-Phosphate: I. The Phosphorolysis and Resynthesis of Purine Desoxyribose Nucleoside. *J. Biol. Chem.* **1950**, *184* (2), 437–448.

(20) Kaspar, F.; Giessmann, R. T.; Neubauer, P.; Wagner, A.; Gimpel, M. Thermodynamic Reaction Control of Nucleoside Phosphorolysis. *Adv. Synth. Catal.* **2020**, *362* (4), 867–876. https://doi.org/10.1002/adsc.201901230.

(21) Alexeev, C. S.; Kulikova, I. V; Gavryushov, S.; Tararov, V. I.; Mikhailov, S. N. Quantitative Prediction of Yield in Transglycosylation Reaction Catalyzed by Nucleoside Phosphorylases. *Adv. Synth. Catal.* **2018**, *360* (16), 3090–3096. https://doi.org/10.1002/adsc.201800411.

(22) Barai, V. N.; Zinchenko, A. I.; Eroshevskaya, L. A.; Kalinichenko, E. N.; Kulak, T. I.; Mikhailopulo, I. A. A Universal Biocatalyst for the Preparation of Base- and Sugar-Modified Nucleosides via an Enzymatic Transglycosylation. *Helv. Chim. Acta* **2002**, *85* (7), 1901–1908. https://doi.org/10.1002/1522-2675(200207)85:7<1901::AID-HLCA1901>3.0.CO;2-C.

(23) Robescu, M. S.; Serra, I.; Terreni, M.; Ubiali, D.; Bavaro, T. A Multi-Enzymatic Cascade Reaction for the Synthesis of Vidarabine 5′-Monophosphate. *Catalysts* **2020**, *10* (1). https://doi.org/10.3390/catal10010060.

(24) Hellendahl, K. F.; Kaspar, F.; Zhou, X.; Yang, Z.; Huang, Z.; Neubauer, P.; Kurreck, A. Optimized Biocatalytic Synthesis of 2-Selenopyrimidine Nucleosides by Transglycosylation. *ChemBioChem* **2021**, *22* (11), 2002–2009. https://doi.org/https://doi.org/10.1002/cbic.202100067.

(25) Pal, S.; Nair, V. Enzymatic Synthesis of Thymidine Using Bacterial Whole Cells and Isolated Purine Nucleoside Phosphorylase. *Biocatal. Biotransformation* **1997**, *15* (2), 147–158. https://doi.org/10.3109/10242429709003615.

(26) Hori, N.; Watanabe, M.; Sunagawa, K.; Uehara, K.; Mikami, Y. Production of 5-Methyluridine by Immobilized Thermostable Purine Nucleoside Phosphorylase and Pyrimidine Nucleoside Phosphorylase from *Bacillus Stearothermophilus* JTS 859. *J. Biotechnol.* **1991**, *17* (2), 121–131. https://doi.org/https://doi.org/10.1016/0168-1656(91)90003-E.

(27) Eilert, L.; Schallmey, A.; Kaspar, F. UV-Spectroscopic Detection of (Pyro-)Phosphate with the PUB Module. *Anal. Chem.* **2022**, *94* (8), 3432–3435. https://doi.org/10.1021/acs.analchem.1c05356.

(28) van den Berg, R.; Peters, J. A.; van Bekkum, H. The Structure and (Local) Stability Constants of Borate Esters of Mono- and Di-Saccharides as Studied by ^{11}B and ^{13}C NMR Spectroscopy. *Carbohydr. Res.* **1994**, *253*, 1–12. https://doi.org/https://doi.org/10.1016/0008-6215(94)80050-2.

(29) Quirino, J. P. CZE and ESI-MS of Borate-Sugar Complexes. *Chromatographia* **2010**, *72* (5), 503–510. https://doi.org/10.1365/s10337-010-1685-8.

(30) Nam-Hee, K.; Hye-Jung, K.; Dong-Il, K.; Ki-Woong, J.; Jung-Kul, L.; Yangmee, K.; Deok-Kun, O. Conversion Shift of D-Fructose to D-Psicose for Enzyme-Catalyzed Epimerization by Addition of Borate. *Appl. Environ. Microbiol.* **2008**, *74* (10), 3008–3013. https://doi.org/10.1128/AEM.00249-08.

(31) Kim, Y.-S.; Kim, J.-E.; Oh, D.-K. Borate Enhances the Production of Lactulose from Lactose by Cellobiose 2-Epimerase from *Caldicellulosiruptor Saccharolyticus*. *Bioresour. Technol.* **2013**, *128*, 809–812. https://doi.org/https://doi.org/10.1016/j.biortech.2012.10.060.

(32) Salonen, N.; Salonen, K.; Leisola, M.; Nyyssölä, A. D-Tagatose Production in the Presence of Borate by Resting *Lactococcus Lactis* Cells Harboring *Bifidobacterium Longuml*-Arabinose Isomerase. *Bioprocess Biosyst. Eng.* **2013**, *36* (4), 489–497. https://doi.org/10.1007/s00449-012-0805-2.

(33) Sun, Z.; Miao, T.; Yin, A.; Qiu, H.; Xiao, Y.; Li, Y.; Hai, J.; Xu, B. Optimization of Fermentation Conditions for Production of L-Arabinose Isomerase of *Lactobacillus Plantarum* WU14. *Food Sci. Nutr.* **2021**, *9* (1), 230–243. https://doi.org/https://doi.org/10.1002/fsn3.1989.

(34) Zhang, Y.-W.; Jeya, M.; Lee, J.-K. L-Ribulose Production by an *Escherichia Coli* Harboring l-Arabinose Isomerase from *Bacillus Licheniformis*. *Appl. Microbiol. Biotechnol.* **2010**, *87* (6), 1993–1999. https://doi.org/10.1007/s00253-010-2600-9.

(35) Smith, K. W.; Johnson, S. L. Borate Inhibition of Yeast Alcohol Dehydrogenase. *Biochemistry* **1976**, *15* (3), 560–565. https://doi.org/10.1021/bi00648a016.

(36) Kim, D. H.; Hee, S. Q.; Norris, A. J.; Faull, K. F.; Eckhert, C. D. Boric Acid Inhibits Adenosine Diphosphate-Ribosyl Cyclase Non-Competitively. *J. Chromatogr. A* **2006**, *1115* (1), 246–252. https://doi.org/https://doi.org/10.1016/j.chroma.2006.02.066.

(37) Giessmann, R. T.; Krausch, N.; Kaspar, F.; Cruz Bournazou, N. M.; Wagner, A.; Neubauer, P.; Gimpel, M. Dynamic Modelling of Phosphorolytic Cleavage Catalyzed by Pyrimidine-Nucleoside Phosphorylase. *Processes* **2019**, *7* (6), 380. https://doi.org/10.3390/pr7060380.

(38) Zhou, X.; Szeker, K.; Janocha, B.; Böhme, T.; Albrecht, D.; Mikhailopulo, I. A.; Neubauer, P. Recombinant Purine Nucleoside Phosphorylases from Thermophiles: Preparation, Properties and Activity towards Purine and Pyrimidine Nucleosides. *FEBS J.* **2013**, *280* (6), 1475–1490. https://doi.org/10.1111/febs.12143.

(39) Kaspar, F.; Wolff, D. S.; Neubauer, P.; Kurreck, A.; Arcus, V. L. pH-Independent Heat Capacity Changes during Phosphorolysis Catalyzed by the Pyrimidine Nucleoside Phosphorylase from *Geobacillus Thermoglucosidasius*. *Biochemistry* **2021**, *60* (20), 1573–1577. https://doi.org/10.1021/acs.biochem.1c00156.

(40) Szeker, K.; Zhou, X.; Schwab, T.; Casanueva, A.; Cowan, D.; Mikhailopulo, I. A.; Neubauer, P. Comparative Investigations on Thermostable Pyrimidine Nucleoside Phosphorylases from *Geobacillus Thermoglucosidasius* and *Thermus Thermophilus*. *J. Mol. Catal. B Enzym.* **2012**, *84*, 27–34. https://doi.org/10.1016/j.molcatb.2012.02.006.

(41) Kaspar, F.; Giessmann, R. T.; Westarp, S.; Hellendahl, K. F.; Krausch, N.; Thiele, I.; Walczak, M. C.; Neubauer, P.; Wagner, A. Spectral Unmixing-Based Reaction Monitoring of Transformations between Nucleosides and Nucleobases. *ChemBioChem* **2020**, *21* (18), 2604. https://doi.org/10.1002/cbic.202000204.

(42) Kaspar, F.; Giessmann, R. T.; Krausch, N.; Neubauer, P.; Wagner, A.; Gimpel, M. A UV/Vis Spectroscopy-Based Assay for Monitoring of Transformations Between Nucleosides and Nucleobases. *Methods Protoc.* **2019**, *2* (3), 60. https://doi.org/10.3390/mps2030060.

(43) Kaspar, F.; Brandt, F. Supplementary Material Nucleoside Borate Esters. **2022**, https://doi.org/10.5281/zenodo.6415158.

(44) Šponer, J. E.; Sumpter, B. G.; Leszczynski, J.; Šponer, J.; Fuentes-Cabrera, M. Theoretical Study on the Factors Controlling the Stability of the Borate Complexes of Ribose, Arabinose, Lyxose, and Xylose. *Chem. – A Eur. J.* **2008**, *14* (32), 9990–9998. https://doi.org/https://doi.org/10.1002/chem.200800961.

(45) Li, Q.; Ricardo, A.; Benner, S. A.; Winefordner, J. D.; Powell, D. H. Desorption/Ionization on Porous Silicon Mass Spectrometry Studies on Pentose−Borate Complexes. *Anal. Chem.* **2005**, *77* (14), 4503–4508. https://doi.org/10.1021/ac050258d.

(46) Amaral, A. F.; Marques, M. M.; da Silva, J. A. L.;

Fraústo da Silva, J. J. R. Interactions of D-Ribose with Polyatomic Anions, and Alkaline and Alkaline-Earth Cations: Possible Clues to Environmental Synthesis Conditions in the Pre-RNA World. *New J. Chem.* **2008**, *32* (11), 2043–2049. https://doi.org/10.1039/B809636H.

(47) Kim, D. H.; Faull, K. F.; Norris, A. J.; Eckhert, C. D. Borate–Nucleotide Complex Formation Depends on Charge and Phosphorylation State. *J. Mass Spectrom.* **2004**, *39* (7), 743–751. https://doi.org/https://doi.org/10.1002/jms.645.

(48) Kim, D. H.; Marbois, B. N.; Faull, K. F.; Eckhert, C. D. Esterification of Borate with NAD^+ and NADH as Studied by Electrospray Ionization Mass Spectrometry and 11B NMR Spectroscopy. *J. Mass Spectrom.* **2003**, *38* (6), 632–640. https://doi.org/https://doi.org/10.1002/jms.476.

(49) Barbeyron, R.; Vasseur, J.-J.; Smietana, M. PH-Controlled DNA- and RNA-Templated Assembly of Short Oligomers. *Chem. Sci.* **2015**, *6* (1), 542–547. https://doi.org/10.1039/C4SC03028A.

(50) Martin, A. R.; Barvik, I.; Luvino, D.; Smietana, M.; Vasseur, J.-J. Dynamic and Programmable DNA-Templated Boronic Ester Formation. *Angew. Chemie Int. Ed.* **2011**, *50* (18), 4193–4196. https://doi.org/https://doi.org/10.1002/anie.201007170.

(51) Bull, S. D.; Davidson, M. G.; van den Elsen, J. M. H.; Fossey, J. S.; Jenkins, A. T. A.; Jiang, Y.-B.; Kubo, Y.; Marken, F.; Sakurai, K.; Zhao, J.; James, T. D. Exploiting the Reversible Covalent Bonding of Boronic Acids: Recognition, Sensing, and Assembly. *Acc. Chem. Res.* **2013**, *46* (2), 312–326. https://doi.org/10.1021/ar300130w.

(52) Stephens, P. J.; Devlin, F. J.; Chabalowski, C. F.; Frisch, M. J. *Ab Initio* Calculation of Vibrational Absorption and Circular Dichroism Spectra Using Density Functional Force Fields. *J. Phys. Chem.* **1994**, *98* (45), 11623–11627. https://doi.org/10.1021/j100096a001.

(53) Becke, A. D. Density-functional Thermochemistry. III. The Role of Exact Exchange. *J. Chem. Phys.* **1993**, *98* (7), 5648–5652. https://doi.org/10.1063/1.464913.

(54) Lee, C.; Yang, W.; Parr, R. G. Development of the Colle-Salvetti Correlation-Energy Formula into a Functional of the Electron Density. *Phys. Rev. B* **1988**, *37* (2), 785–789. https://doi.org/10.1103/PhysRevB.37.785.

(55) Van Lenthe, E.; Baerends, E. J. Optimized Slater-Type Basis Sets for the Elements 1–118. *J. Comput. Chem.* **2003**, *24* (9), 1142–1156. https://doi.org/https://doi.org/10.1002/jcc.10255.

(56) Klamt, A.; Schüürmann, G. COSMO: A New Approach to Dielectric Screening in Solvents with Explicit Expressions for the Screening Energy and Its Gradient. *J. Chem. Soc. Perkin Trans. 2* **1993**, No. 5, 799–805. https://doi.org/10.1039/P29930000799.

(57) Ishii, T.; Ono, H. NMR Spectroscopic Analysis of the Borate Diol Esters of Methyl Apiofuranosides. *Carbohydr. Res.* **1999**, *321* (3), 257–260. https://doi.org/https://doi.org/10.1016/S0008-6215(99)00184-6.

(58) Okano, T.; Komatsu, T.; Nara, T.; Tsuji, K. Solubilization of Purine Nucleosides by a Borate and Its Mechanism : Electronic Properties of N-Heteroaromatics. XXIX. *Yakugaku zasshi* **1969**, *89* (1), 51–57. https://doi.org/10.1248/yakushi1947.89.1_51.

(59) Van Der Spoel, D.; Lindahl, E.; Hess, B.; Groenhof, G.; Mark, A. E.; Berendsen, H. J. C. GROMACS: Fast, Flexible, and Free. *J. Comput. Chem.* **2005**, *26* (16), 1701–1718. https://doi.org/https://doi.org/10.1002/jcc.20291.

(60) Lindahl, E.; Abraham, M. J.; Hess, B.; Van Der Spoel, D. GROMACS 2020.3 Source Code. **2020**, https://doi.org/10.5281/zenodo.3923645.

(61) Huang, J.; MacKerell Jr, A. D. CHARMM36 All-Atom Additive Protein Force Field: Validation Based on Comparison to NMR Data. *J. Comput. Chem.* **2013**, *34* (25), 2135–2145. https://doi.org/https://doi.org/10.1002/jcc.23354.

(62) Sidorov-Biryukov, D. D.; Podshivalov, D. D.; Timofeev, V. I.; Zhukhlistova, N. E.; Kuranova, I. P. Molecular Dynamics Study of Thymidine Phosphorylase from *E. Coli* in the Apo Form and in Complexes with Substrates. *Crystallogr. Reports* **2019**, *64* (1), 98–104. https://doi.org/10.1134/S1063774518060287.

(63) Mendieta, J.; Martín-Santamaría, S.; Priego, E.-M.; Balzarini, J.; Camarasa, M.-J.; Pérez-Pérez, M.-J.; Gago, F. Role of Histidine-85 in the Catalytic Mechanism of Thymidine Phosphorylase As Assessed by Targeted Molecular Dynamics Simulations and Quantum Mechanical Calculations. *Biochemistry* **2004**, *43* (2), 405–414. https://doi.org/10.1021/bi034793o.

(64) Omari, K. E.; Bronckaers, A.; Liekens, S.; Pérez-Pérez, M.-J.; Balzarini, J.; Stammers, D. K. Structural Basis for Non-Competitive Product Inhibition in Human Thymidine Phosphorylase: Implications for Drug Design. *Biochem. J.* **2006**, *399* (2), 199–204. https://doi.org/10.1042/BJ20060513.

(65) Gao, X.-F.; Huang, X.-R.; Sun, C.-C. Role of Each Residue in Catalysis in the Active Site of Pyrimidine Nucleoside Phosphorylase from *Bacillus Subtilis*: A Hybrid QM/MM Study. *J. Struct. Biol.* **2006**, *154* (1), 20–26. https://doi.org/https://doi.org/10.1016/j.jsb.2005.11.014.

(66) Tozer, T.; Heale, K.; Manto Chagas, C.; de Barros, A. L. B.; Alisaraie, L. Interdomain Twists of Human Thymidine Phosphorylase and Its Active–Inactive Conformations: Binding of 5-FU and Its Analogues to Human Thymidine Phosphorylase versus Dihydropyrimidine Dehydrogenase. *Chem. Biol. Drug Des.* **2019**, *94* (5), 1956–1972. https://doi.org/https://doi.org/10.1111/cbdd.13596.

(67) Pugmire, M. J.; Cook, W. J.; Jasanoff, A.; Walter, M. R.; Ealick, S. E. Structural and Theoretical Studies Suggest Domain Movement Produces an Active Conformation of Thymidine Phosphorylase. *J. Mol. Biol.* **1998**, *281* (2), 285–299. https://doi.org/10.1006/jmbi.1998.1941.

(68) Rick, S. W.; Abashkin, Y. G.; Hilderbrandt, R. L.; Burt, S. K. Computational Studies of the Domain Movement and the Catalytic Mechanism of Thymidine Phosphorylase. *Proteins Struct. Funct. Bioinforma.* **1999**, *37* (2), 242–252. https://doi.org/https://doi.org/10.1002/(SICI)1097-0134(19991101)37:2<242::AID-PROT9>3.0.CO;2-5.

(69) Kulikova, I. V; Drenichev, M. S.; Solyev, P. N.; Alexeev, C. S.; Mikhailov, S. N. Enzymatic Synthesis of 2-Deoxyribose 1-Phosphate and Ribose 1 Phosphate and Subsequent Preparation of Nucleosides. *European J. Org. Chem.* **2019**, *2019* (41), 6999–7004. https://doi.org/10.1002/ejoc.201901454.

(70) Kaspar, F.; Neubauer, P.; Kurreck, A. Kinetic Analysis of the Hydrolysis of Pentose-1-Phosphates through Apparent Nucleoside Phosphorolysis Equilibrium Shifts. *ChemPhysChem* **2021**, *22* (3), 283–287. https://doi.org/https://doi.org/10.1002/cphc.202000901.

(71) Kamel, S.; Weiß, M.; Klare, H. F. T.; Mikhailopulo, I. A.; Neubauer, P.; Wagner, A. Chemo-Enzymatic Synthesis of α-D-Pentofuranose-1-Phosphates Using Thermostable Pyrimidine Nucleoside Phosphorylases. *Mol. Catal.* **2018**, *458*, 52–59. https://doi.org/10.1016/j.mcat.2018.07.028.